(12) INTERNATIONAL APPLICATION PUBLISHED UNDER THE PATENT COOPERATION TREATY (PCT)

(19) World Intellectual Property Organization
International Bureau

(43) International Publication Date
9 February 2012 (09.02.2012)

PCT

(10) International Publication Number
WO 2012/019172 A1

(51) **International Patent Classification**:
A61B 8/00 (2006.01)

(21) **International Application Number**:
PCT/US2011/046865

(22) **International Filing Date**:
5 August 2011 (05.08.2011)

(25) **Filing Language**: English

(26) **Publication Language**: English

(30) **Priority Data**:
61/371,647 6 August 2010 (06.08.2010) US
61/371,982 9 August 2010 (09.08.2010) US

(71) **Applicant** *(for all designated States except US)*: **THE TRUSTEES OF COLUMBIA UNIVERSITY IN THE CITY OF NEW YORK** [US/US]; 412 Low Memorial Library, 535 West 116th Street, Mail Code 4308, New York, NY 10027 (US).

(72) **Inventors; and**
(75) **Inventors/Applicants** *(for US only)*: **BORDEN, Mark A.** [US/US]; 2300 Arapahoe Avenue, #110, Boulder, CO 80302 (US). **FESHITAN, Jameel A.** [GB/US]; 110 Morningside Drive, Apt.46, New York, NY 10027 (US). **KONOFAGOU, Elisa E.** [GR/US]; 101 West End Avenue, Apt #25G, New York, NY 10023 (US). **VLACHOS, Fotis** [GR/GR]; 1 Maravelia street, Iliopolis, Attiki 16341 (GR).

(74) **Agents**: **CATAN, Mark A.** et al.; Miles & Stockbridge P.C., 1751 Pinnacle Drive, Suite 500, McLean, VA 22102-3833 (US).

(81) **Designated States** *(unless otherwise indicated, for every kind of national protection available)*: AE, AG, AL, AM, AO, AT, AU, AZ, BA, BB, BG, BH, BR, BW, BY, BZ, CA, CH, CL, CN, CO, CR, CU, CZ, DE, DK, DM, DO, DZ, EC, EE, EG, ES, FI, GB, GD, GE, GH, GM, GT, HN, HR, HU, ID, IL, IN, IS, JP, KE, KG, KM, KN, KP, KR, KZ, LA, LC, LK, LR, LS, LT, LU, LY, MA, MD, ME, MG, MK, MN, MW, MX, MY, MZ, NA, NG, NI, NO, NZ, OM, PE, PG, PH, PL, PT, QA, RO, RS, RU, SC, SD, SE, SG, SK, SL, SM, ST, SV, SY, TH, TJ, TM, TN, TR, TT, TZ, UA, UG, US, UZ, VC, VN, ZA, ZM, ZW.

(84) **Designated States** *(unless otherwise indicated, for every kind of regional protection available)*: ARIPO (BW, GH, GM, KE, LR, LS, MW, MZ, NA, SD, SL, SZ, TZ, UG, ZM, ZW), Eurasian (AM, AZ, BY, KG, KZ, MD, RU, TJ, TM), European (AL, AT, BE, BG, CH, CY, CZ, DE, DK, EE, ES, FI, FR, GB, GR, HR, HU, IE, IS, IT, LT, LU,

[Continued on next page]

(54) **Title**: MEDICAL IMAGING CONTRAST DEVICES, METHODS, AND SYSTEMS

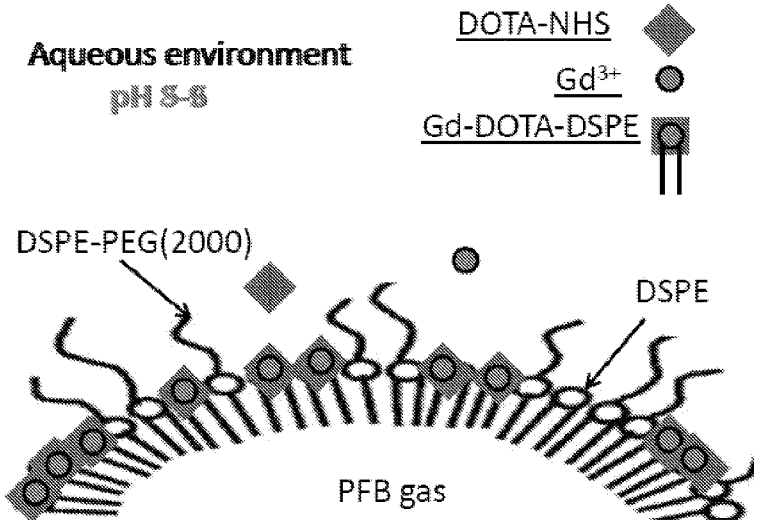

FIG. 9

(57) **Abstract**: Systems, methods, and devices for generating and using size-selected lanthanide-coated microbubbles for controlling an imaging signal via microbubble fragmentation and for magnetic resonance imaging guided focused ultrasound therapy.

WO 2012/019172 A1

LV, MC, MK, MT, NL, NO, PL, PT, RO, RS, SE, SI, SK, SM, TR), OAPI (BF, BJ, CF, CG, CI, CM, GA, GN, GQ, GW, ML, MR, NE, SN, TD, TG).

Published:

— *with international search report (Art. 21(3))*

— *before the expiration of the time limit for amending the claims and to be republished in the event of receipt of amendments (Rule 48.2(h))*

MEDICAL IMAGING CONTRAST DEVICES, METHODS, AND SYSTEMS

CROSS-REFERENCE TO RELATED APPLICATIONS

This application is an International Application, which claims priority to and the benefit of U.S. Provisional Application Nos. 61/371,647, filed on August 6, 2010, and 61/371,982, filed on August 9, 2010, the contents of which are incorporated herein by reference in their entireties.

STATEMENT REGARDING FEDERALLY SPONSORED RESEARCH

This invention was made with government support under Grant No. RO1EB9041 awarded by National Institute of Health. The government has certain rights in this invention.

FIELD

The present disclosure is directed to medical imaging contrast devices, systems, and methods, and, more particularly to methods, systems, and devices for medical imaging contrast using lanthanide-coated microbubbles and methods, systems, and devices for magnetic resonance imaging guided focused ultrasound therapy (MRIg-FUS).

SUMMARY

A paramagnetic lanthanide ion, such as gadolinium (Gd^{3+}), can be loaded through chelation to a macrocyclic molecule onto a lipid shell of a microbubble. The intrinsic gas/liquid interface of the microbubble can cause a local inhomogeneity in the magnetic field. This inhomogeneity can induce a magnetic susceptibility difference, which can be used to generate a negative contrast in a magnetic resonance image (MRI) where the image is weighted by longitudinal relaxation (R1). When the microbubble is intact with a gas core (and therefore a gas/liquid interface) the contrast enhancement may be minimal. However, when the microbubble is fragmented and the gas core is dissolved, the fragmented shell of the microbubble that is left behind can create a positive contrast in the image weighted by R1. Thus, the lanthanide-coated microbubble can allow detection of the location and intensity of ultrasound-induced microbubble destruction, for example, during MRI-guided ultrasound therapies, such as MRI-guided high-intensity focused ultrasound therapies. Monitoring of such therapies can thereby be improved while reducing negative side effects.

BRIEF DESCRIPTION OF THE DRAWINGS

Fig. 1 is a graphical representation of number and volume size distribution of polydisperse microbubbles according to an embodiment of the disclosed subject matter;

Fig. 2 is a schematic representation of separation by centrifugation according to an embodiment of the disclosed subject matter;

Fig. 3 is a schematic representation of microbubble size isolation according to an embodiment of the disclosed subject matter;

Fig. 4 is a schematic representation of microbubble size separation according to an embodiment of the disclosed subject matter;

Fig. 5 is a graphical representation of size distribution of three exemplary size-sorted microbubble populations;

Fig. 6 is an exemplary comparison of T1 times of gadolinium bound and unbound microbubbles.

Figs. 7-8 are exemplary relaxation rates for intact and destroyed microbubbles;

Fig. 9 is a schematic representation of a post-labeled microbubble.

DETAILED DESCRIPTION

Magnetic resonance imaging (MRI) and ultrasound imaging using microbubbles can be used as imaging modalities in diagnostic and drug therapy applications. Both imaging modalities may utilize contrast agents to enhance

the signal to contrast ratio. MRI relies on the examination of different distribution and properties of water in observed tissues as well as the spatial variation of longitudinal (T1) and transversal (T2) relaxation times after excitation with a radio frequency pulse to produce images. MRI signal increases with 1/T1 and decreases with 1/T2. T1-weighted MRI has been more commonly used in the clinical setting.

The MRI contrast agents can be classified according to the relaxation processes they enhance. In particular, R1 (1/T1) contrast agents include paramagnetic materials, such as gadolinium ions (Gd^{3+}) or other lanthanide ions. The R1 contrast agents act to reduce the T1 time thereby producing positive contrast (i.e., brighter image). The R2 (1/T2) contrast agents reduce the T2 times and thus produce a negative contrast (i.e., darker image). Contrast agents that increase the ratio of R2/R1 are called susceptibility weighted agents, due to the greater loss of phase coherence caused by inhomogeneities in the magnetic field that produce longer T2 decay times above a normal baseline.

The relaxivity of T1-weighted contrast agents can be increased by binding to macromolecular substrates, such as, but not limited to, liposomes, dendrimers, and nanoparticles. Such complexes act as vesicles to increase loading of the MRI contrast agent and to reduce the tumbling rate of the contrast media so as to allow for a substantial increase in the relaxivity R1.

Gas-filled microbubbles can be used as contrast agents for ultrasound imaging and targeted drug delivery due to their compressible gas cores. As used herein, microbubbles refer to micron-sized spherical gas-filled particles, which can be stabilized by an organic coating, such as a lipid shell, at the gas-

liquid interface. Microbubbles having a diameter of 10 µm or less can be generated and used as contrast agents. The gas cores of the microbubbles provide strong backscatter echo that can be detected using the ultrasound transducer. Depending on controlled ultrasound parameters, the microbubbles may cavitate stably or inertially, thereby allowing for imaging, targeting, controlled release, and vascular permeability enhancement. Microbubbles can also be destroyed by externally applied ultrasound of sufficient intensity so as to release shell material as well as any gas contained by the microbubble shell.

Microbubbles can also be used as magnetic resonance susceptibility contrast agents (i.e., reducing R1) *in vivo* due to the induction of large local magnetic susceptibility differences by the gas-liquid interface, thereby creating a negative contrast in the MRI image. This feature of the microbubbles described herein allows them to be utilized as ultrasound-triggered MRI contrast agents. The MRI signal can be spatially and temporally controlled via microbubble destruction by external acoustic forces, since the susceptibility-weighted (i.e., negative contrast) should disappear, or at least be reduced, with the destruction of the gas-liquid interface of the microbubble. Moreover, lanthanide ions that coated the microbubble remain with the now-destroyed lipid shell. Thus, the positive contrast can increase due to the presence of the paramagnetic contrast agent on the remnants of the microbubble shell. The resulting MRI image can evolve from a normal tissue contrast before microbubble destruction to a positive contrast after microbubble destruction.

Microbubble populations having different diameters or sizes can be isolated by centrifugation. These size-selected microbubbles can provide

superior performance over polydisperse microbubble populations in imaging and biomedical applications, such as MRI-guided focused ultrasound (MRIg-FUS) therapy. For example, microbubbles can be sorted into size ranges of 1-2 µm, 4-5 µm, and 6-8 µm in diameter from an initially polydisperse suspension. The sorting of the microbubbles into separate size-based populations can be achieved by, for example, centrifugation. For a given centrifugal speed, a two-phase separation can occur, with the upper phase containing primarily larger microbubbles and the lower phase containing the less buoyant, smaller microbubbles. The larger microbubbles can have a faster rise velocity at a given centrifugal force than the smaller ones. The separation process can be adjusted for different microbubble populations by varying parameters, such as centrifugation speed, centrifugation time, column height, and initial suspension fraction.

Lipid-coated microbubbles can be prepared in high concentrations by acoustic emulsification of a suspension containing a mixture of a phospholipid and a lipo-polymer in the presence of an insoluble gas. For example, the phospholipid may be 1, 2-distearoyl-*sn*-glycero-3-phosphoethanolamine (DSPE), the lipo-polymer may be 1,2-distearoyl-*sn*-glycero-3-phosphoethanolamine-N-[methoxy(polyethylene glycol)-2000] (DSPE-PEG2000), and the insoluble gas may be perfluorobutane.

Microbubbles can be coated with DSPE and DSPE-PEG2000 at a molar ratio of 9:1. The indicated amount of DSPE can be dissolved in a chloroform/methanol/water mixture and transferred to a container, such as a glass vial. The organic solvent mixture can then be evaporated with a steady

stream of, for example, nitrogen while vortexing for 10 minutes followed by several hours under vacuum. 0.01 M NaCl phosphate-buffered saline (PBS) solution can be filtered using a 0.2-µm pore size polycarbonate filter. The dried lipid film can then be hydrated with the filtered PBS and mixed with DSPE-PEG2000 (e.g., 25 mg/mL in filtered PBS) to a final lipid concentration of 2.0 mg/mL.

The lipid mixture can be first sonicated with, for example, a 20-kHz probe at low power (e.g., approximately 3W) in order to heat the pre-microbubble suspension above the main phase transition temperature of the phospholipid (e.g., for DSPE about 74°C) and further disperse the lipid aggregates into small unilamellar liposomes. PFB gas can then be introduced by flowing it over the surface of the lipid suspension. Subsequently, high power sonication (e.g., approximately 33W) can be applied to the suspension for about 10 seconds at the gas-liquid interface to generate microbubbles therein. Of course, other microbubble fabrication techniques may also be used to form the microbubbles described herein.

The initial microbubble population can be determined by light extinction. FIG. 1 shows number % and volume % of an exemplary polydisperse population of microbubbles after acoustic emulsification as a function of diameter. As is evident from the number-weighted distribution of FIG. 1 the larger diameter size microbubbles are present in the polydisperse population to a lesser degree than the smaller sizes after emulsification.

Centrifugation can be used to select microbubbles having a certain diameter from other microbubbles based on their migration in a centrifugal field,

as illustrated schematically in FIG. 2. Centrifugation conditions can be determined based on initial microbubble size distribution and concentration. For a given initial size distribution, time period, and syringe column length, the strength of the centrifugal field (in RCF) can be calculated using the following equations:

$$u_i = \frac{2(\rho_2 - \rho_{1i})}{9\mu} R_i^2 g \quad , \tag{1}$$

$$\frac{\mu_2^*}{\mu_2} = 1 + 2.5\Phi + 7.6\Phi^2 , \tag{2}$$

$$\Phi = \sum_{i=1}^{N_d} \Phi_i , \tag{3}$$

where Φ is the total microbubble volume fraction for N size classes, R_i is the particle radius, g is gravity, μ is viscosity, ρ_2 is the density of the fluid, ρ_{1i} is the density of the particulate, and i refers to the particle size class. Volume fraction can be assumed constant over the entire column and acceleration/deceleration effects can be neglected.

Following production, microbubbles can be collected into syringes, for example 30 mL syringes having a length of approximately 8.2 cm. Larger size class microbubbles (e.g., diameters greater than 1 µm) can be separated from submicron particles and vesicles by applying centrifugal force using a bucket-rotor centrifuge, for example, such that 1 µm bubbles rise from the bottom to the top of the column. Centrifugation at 300 RCF (relative centrifugal force) for 5 minutes was performed to collect all microbubbles from the suspension into a cake resting against the syringe plunger. The resulting concentrated

microbubble cake can then be re-dispersed into 30 mL of filtered phosphate buffered saline (PBS) solution and the infranatant discarded. The initial suspension volume fraction can be adjusted to 5-10%. A schematic of a protocol that can be used for determining the RCF for size selection is illustrated in FIG. 3.

For a specific microbubble size, the calculated RCF needed for the microbubbles to rise from the bottom to the top of the syringe column is applied to the polydisperse solution for a predetermined period of time, e.g., one minute. After centrifugation, microbubbles above the specified size will be incorporated into the cake, while a fraction of the total microbubbles less than the desired cutoff will remain in the infranatant, as schematically illustrated in FIG. 4.

For the selection of smaller microbubble populations (e.g., 1-2 μm in diameter), the infranatant can be kept and concentrated. For the selection of microbubbles of larger size (e.g., greater than 2 μm in diameter), the process can employ multiple steps. For example, in selecting the 4-5 μm diameter microbubble population, the population of microbubbles having diameters less than 4 μm can be removed from the polydisperse solution by repeated centrifugation cycles at calculated RCF and discarding the infranatant after each cycle. Multiple cycles of centrifugation, e.g., 5-8 cycles, may be necessary in order to remove substantially all of the smaller microbubbles from the desired larger size microbubble population. After isolating the microbubbles having diameters greater than 4 μm, the population of microbubbles having diameters greater than 5 μm can be removed from the solution. The cake from the first step, which includes microbubbles having diameters greater than 4 μm, can be

re-suspended. The RCF calculated for 5 µm diameter microbubbles to rise to the top of the column can then be applied to the suspension. The infranatant, which includes microbubbles having a diameter in the 4-5 µm range, can be kept and concentrated. A similar protocol can be applied to microbubbles of any desired size range, such as 6-8 µm diameter microbubbles. FIG. 5 shows the size distribution (in number percentage and volume percentage) of three exemplary size-sorted microbubbles populations separated using the above process. Microbubble size distribution can be determined by laser light obscuration and scattering.

For microbubbles to be useful for MRIg-FUS as well as other applications, it would be helpful to their performance if the microbubble populations maintained their size distribution and are otherwise stable. Stability affects shelf life and biodistribution. The degradation of microbubble suspensions can be attributed to Ostwald's ripening, which is the process by which large particles can grow at the expense of smaller ones. Ostwald's ripening is driven by the differences in solubility due to differences in curvature of particles. Small particles shrink due to enhanced solubility arising from their high curvature while larger particles grow. The ripening process can reach a stationary regime, where the form of the particle size distribution is achieved. In this regime, particle growth may be linear with respect to time, and the number average radius can be equivalent to the critical radius of particle growth. A microbubble particle may grow if it is above the critical radius, whereas microbubbles below the critical radius may shrink. The growth (or shrinkage) rate of microbubbles may be affected by surfactant type, the presence of vesicles, as the polydispersity of the microbubbles.

Ostwald's ripening is driven by differences in solubility of different emulsion radii. Thus, a polydisperse microbubble population may ripen at a more appreciable rate than a substantially monodisperse microbubble population. Size-selected microbubble populations may maintain their size distribution better than polydisperse suspensions. Moreover, as the microbubble radii more closely approach the critical radii, the growth rate of the microbubbles may get closer to zero.

The rate of ripening may also depend on surfactant concentration. For example, sodium dodecyl sulphate (SDS) and a phospholipid surfactant may be used to alter the rate of ripening. SDS is a soluble surfactant whose surface tension (e.g., 30 mM/m) can be assumed constant above its critical micelle concentration (CMC). In contrast, the surface tension of the phospholipid surfactant on a microbubble is not constant such that the surface tension changes as the microbubble shrinks or expands. Above their CMC, the surfactants may form vesicles. Due to different shape factors, SDS tends to form micelles while phospholipids tend to form bilayers. These vesicles and micelles may also influence the growth rate of the microbubble populations.

MRI-detectable microbubbles can be designed for MRIg-FUS therapy. MRIg-FUS therapy utilizes high intensity focused ultrasound (HIFU) to ablate tissue and MRI to monitor the thermal dosage applied. Applications for MRIg-FUS include, but are not limited to, monitoring the heating of muscle tissue during (HIFU) and treatment of uterine fibroids, as well as treatment of liver-, bone-, prostate-, and brain-related diseases. In addition to heating, ultrasound can produce other therapeutic bioeffects. At high acoustic intensities,

microbubbles may be formed in the focal area during the rarefaction phase of the ultrasound wave by inception cavitation. These bubbles may grow unstably and undergo transient collapse, or inertial cavitation, producing jets and shockwaves that enhance heating at the focus. However, the formation of these inception microbubbles can be unpredictable, and inertial cavitation may lead to damage of tissue outside the desired region.

In MRIg-FUS, the potential for damage can be reduced by using preformed lipid-coated microbubbles, such as the microbubbles described herein. These microbubbles can have a lower acoustic intensity threshold for ablation, thereby minimizing the thermal buildup of heat in surrounding tissue that can be associated with high intensity focused ultrasound (HIFU). Moreover, the lipid-coated microbubbles can be used as a contrast agent for ultrasound imaging due to their compressible gas cores, which render the microbubbles echogenic. Depending on ultrasound parameters, the lipid-coated microbubbles may cavitate stably or inertially thereby allowing for imaging, targeting, controlled release of microbubble payloads (e.g., the gas core of the microbubble), and vascular permeability enhancement. The microbubbles may also enhance drug delivery via contract stress due to gas expansion or shear stress due to liquid flow around the microbubble.

One application for MRIg-FUS with microbubbles is in the opening of the Blood-Brain-Barrier (BBB). The BBB acts a permeability barrier in the blood capillary endothelium that prevents most molecules in the blood greater than 400 Da from penetrating into the brain. Since many drugs are greater than 400 Da, the BBB effectively prevents the treatment of neurodegenerative diseases,

such as Parkinson's, Huntington's, and Alzheimer's. However, microbubbles when used with FUS can lead to a localized, noninvasive, and transient opening of the BBB. The opening of the BBB can then be detected by MRI while using an appropriate contrast agent, such as a T1-weighted MRI contrast agent.

For MRIg-FUS therapy applications, a paramagnetic lanthanide, such as gadolinium (Gd^{3+}), can be loaded through chelation to a macrocyclic ligand molecule that is conjugated to the lipid shell of the microbubble. The lanthanide is a contrast agent for T1-weighted MRI whose *in vivo* toxicity can be reduced via the chelation to the macrocyclic ligand. The amount of lanthanide in the microbubble shell can be measured, for example, using optical emission spectroscopy. The relaxivity of the lanthanide can be increased by binding the lanthanide to macromolecular or colloidal substrates, such as, but not limited to, liposomes, dendrimers, and nanoparticles. These complexes increase the relaxivity by slowing down the molecular tumbling rate of the lanthanide. The attachment of the lanthanide to the lipid shell of the microbubble may also slow down the tumbling rate and/or increase τ_R by increasing the rigidity and size of the complex. The centrifugal separation technique described above allows selection of microbubbles having a larger surface area for the attachment of the lanthanide.

The intrinsic gas/liquid interface of the microbubble can also cause a local inhomogeneity in the magnetic field under MRI, which reduces T1 signal and produces a negative contrast (i.e., darker image). The microbubbles can thus act as magnetic resonance susceptibility contrast agents *in vivo* due to the magnetic susceptibility differences at the gas-liquid interface, thereby causing a

positive contrast in T2- and a negative contrast in T1-weighted MRI. The negative T1-contrast nature of the microbubbles allows them to be utilized as ultrasound triggered MRI contrast agents. When the microbubble is intact with a gas core, the contrast enhancement of the lanthanide-bound shell is minimal. However, when the microbubble is fragmented and the gas core is dissolved, the fragmented shell that is left behind can increase the T1 signal, thereby resulting in a positive contrast (i.e., brighter image). The T1-weighted MRI signal can be spatially and temporally controlled via the destruction of the microbubbles by external acoustic forces, since the negative contrast should dissipate with the absence of the gas-liquid interface after microbubble destruction. Moreover, the positive contrast should increase due to the presence of the paramagnetic lanthanide on the remnant shell material. In other words, the image should change from a normal tissue contrast to a positive contrast as the microbubbles are destroyed by externally applied acoustic signals. As a result, lanthanide-bound microbubbles can provide MRI-based detection of the location and dose of focused ultrasound during MRIg-FUS by providing MRI visualization of ultrasound-induced microbubble destruction.

Microbubbles with paramagnetic lanthanide-bound shells can be fabricated using a post-labeling technique. The macrocyclic ligand DOTA-NHS can be conjugated to the amine group of the DSPE in the shell of size-selected microbubbles, followed by chelation of lanthanide.

The lanthanide can be bound to the lipid shell of the microbubbles by functionalizing the microbubble shell with a macrocyclic ligand. The ligand can

react with the primary amino group on the DSPE lipid shell and serves to reduce the *in vivo* toxicity of the lanthanide, which could otherwise block calcium channels *in vivo*. For example, the ligand may be 1,4,7,10-Tetraazacyclododecane-1,4,7,10-tetraacetic acid (DOTA) or 1,4,7,10-Tetraazacylcododecane-1,4,7,10-tetraacetic acid mono(*N*-hydroxysuccinimide ester) (DOTA-NHS).

The ligand DOTA-NHS contains an NHS ester active group, which is a hydrophilic active group that couples rapidly with primary amines on target molecules. The NHS-ester can react with the nucleophilic amine residue to create a stable amide linkage. The microbubble suspension can be buffered to slightly basic conditions to make the primary amine more nucleophilic, thereby increasing its reactivity with the electrophile on DOTA-NHS. NHS esters can have a half-life on the order of hours a physiological pH. However, the amine reactivity and rate of hydrolysis can increase with pH. To minimize the hydrolysis rate, a high concentration of active group amine can be provided by concentrating the microbubble suspension.

The degree of modification to produce optimal product can also be controlled by adjusting the ratio of NHS-esters to target amine molecules. Using microbubble size information, such as obtained via light extinction, the total microbubble surface area in the microbubble population can be calculated. The average projected area per lipid molecule for the lipid DSPE can be approximated as 0.44 nm^2. The total number of lipid molecules on the microbubble shell surface can then be calculated. The relative lipid molar ratio in bulk solution can be approximately the same as for the microbubble shell.

Based on the molar percentage of amine residue, a 50 molar excess amount of NHS-esters can be provided for conjugation.

After conjugation of the metal chelating ligand (e.g., DOTA) to the microbubble shell, the paragmagnetic lanthanide ion (e.g., $Gd^{3+}Z$) can be bound to the microbubble shell via a chelation reaction to form, for example, DSPE-DOTA-Gd. DOTA and a lanthanide such as Gd^{3+} can form a complex with a high thermodynamic stability and low dissociation rate. The rate at which DOTA forms a complex with a lanthanide can depend on many factors including pH, temperature, and concentration of the reactants. An optimal buffer range for this reaction can be within a pH of 5-6, since above pH 6 lanthanides may start to form insoluble hydroxylated species.

Gadolinium forms $Gd(H_2O)_8^{3+}$ in aqueous solution at pH 5-6. During chelation, most of the water molecules are displaced form the inner-sphere of the Gd^{3+} ion by more basic donor atoms of DOTA, including amines (e.g., NH_3) or carboxylates (e.g., COOH) except for one which remains bound to Gd^{3+}. The lone water binding site can be important for MRI contrast since it allows a large number of water molecules to experience the magnetization from Gd^{3+} each second via chemical exchange thereby increasing relaxivity.

The formation of the complex can be a relatively slow process at room temperature, and the rate determining step can involve the base assisted rearrangement of the intermediate complex into the final complex. To increase the rate of complexation, the reaction contents can be heated to a temperature about 5-10° below the main phase transition temperature (T_m) of the lipid component (e.g., for DSPE, T_m = 74°C) for 1-2 hours. Microbubbles coated with

DSPE can be stable at such conditions without substantial change in size distribution and concentration. After the chelation reaction, excess lanthanides can be removed by washing the microbubbles one or more times via centrifugation.

The amount of lanthanide chelated can be determined by, for example, inductively-coupled plasma optical emission spectrometry (ICP-OES). ICP-OES is an analytical technique used for the detection of trace metals. It is a type of emission spectroscopy that uses the inductively coupled plasma to produce excited atoms and ions that emit electromagnetic radiation at wavelengths characteristic of a particular element. The intensity of this emission is indicative of the concentration of the element within the sample. The ICP-OES allows for the determination of the lanthanide concentration within the sample.

As discussed above, the presence of paramagnetic lanthanide, such as Gd^{3+}, on the microbubble shell can reduce the longitudinal relaxation times and produce greater signal strength after microbubble dissolution. Relaxivity of the lanthanide-bound lipid shell can be determined by varying the concentration of the samples and by measuring the T1 relaxation times with de-ionized water as a reference. The T1-weighted relaxivity, r_1, is determined from the slope of the plot of $(1/T1)_{obs}$ versus concentration of the lanthanide on the microbubble shell and is expressed in units of m/(Ms). The T1-weighted relaxivity, r_1, can be calculated from:

$$\left(\frac{1}{T_1}\right)_{obs} = \left(\frac{1}{T_1}\right)_{d} + r_1[Gd], \quad (4)$$

where $(1/T1)_{obs}$ is the observed T1-weighted relaxivity, $(1/T1)_d$ is the diamagnetic contribution or relaxation rate of tissue, $(1/T1)_p$ is the paramagnetic (e.g., Gadolinium) contribution to relaxivity and [Gd] is the concentration of the Gd^{3+}. FIG. 6 shows the T1 times of both 4-5 µm diameter microbubbles containing 30% Gd^{3+} and unbound microbubbles for comparison. As is apparent from the figure, unbound microbubbles reduce the T1 signal whereas Gd-bound microbubbles have minimal effect on contrast enhancement. The application of an ultrasonic destruction pulse to the microbubbles removes the gas-liquid interface, thereby resulting in an increase in the T1 signal due to the remnant shell containing only the paramagnetic Gd-DOTA complex. This is illustrated in the results of FIGS. 7-8, where destroyed microbubbles show a greater normalized relaxation rate than corresponding intact microbubbles. Of course, other imaging or contrast applications for the gas-filled microbubbles beyond the MRIg-FUS application described herein are also possible according to one or more contemplated embodiments.

In an exemplary embodiment, the effect of Gd^{3+}-bound microbubbles on the T_1 and T_2 relaxation times was determined using MR relaxometry. Intact and fragmented Gd^{3+}-bound microbubbles were mixed with saline in four different volume ratios (0, 25, 50 and 100%) creating 200 µL solutions, which were placed in MR-compatible tubes with an inner diameter of 0.5 cm. Intact and fragmented 4-5 µm DOTA-bound microbubbles without Gd^{3+} binding were used as controls. A 9.4 T vertical MRI system (Bruker Biospin, Billerica, MA) was used to acquire turbo spin echo (RARE-VTR) images with variable repetition times (from 300 to 12,500 ms) and multi-slice multi-echo (MSME)

images with variable echo times (from 20 to 320 ms) for T_1 and T_2 mapping, respectively. Eight 1.5 mm-thick, axial slices with a field of view (FOV) of 15×15 mm^2 (matrix size: 96×96) covered the entire solution in each tube. Each slice depicted a slab of all four solutions at a specific height. T_1 and T_2 relaxation maps of each slice were derived using the Image Processing Toolbox of MATLAB R2008b (MathWorks Inc., Natick, MA). The first and last slice were not taken into account in the relaxation measurements, since the MR signal coming from these slices was contaminated by the void below and over the solution. The pixel-by-pixel estimations yielded the T_1 and T_2 maps, respectively. Four pre-defined, identical, circular regions of interest (ROI) of 2.35 mm in diameter were selected on each slice, in order to measure the relaxation rate of each solution throughout the tube. Each ROI covered a large surface area within the limits of the tube. Six measurements were made for each tube (from slice 1 to 6) and the mean value yielded the T_1 or T_2 relaxation times for each solution.

The size isolation protocol yielded 4-5 μm diameter microbubbles at a concentration a least 2 x 10^9 MB/mL. After DOTA conjugation, microbubble concentration and number-weighted median diameter deviated by less than 1%. In this study, chelation reactions were not carried out at room temperature due to the observed lack of adequate Gd^{3+} binding to DOTA at this condition and because the rate of chelation of Gd^{3+} to DOTA was found to increase at elevated temperatures and proton concentrations. After chelation at 50 °C and pH 5.6, microbubble concentration decreased by ~50% while the number-weighted median diameter deviated by less than 1%. After chelation at 70 °C,

however, microbubble concentration decreased by ~65% while the number-weighted median diameter also decreased by ~30%. From ICP-OES analysis, the Gd^{3+} chelation on the microbubble shell occurring at 50 °C and 70 °C was $7.0 \times 10^5 \pm 1.6 \times 10^5$ (mean ± standard deviation) and $7.5 \times 10^5 \pm 3.0 \times 10^5$ ions/μm^2, respectively. Therefore, all subsequent chelation reactions were carried out at 50 °C since the size distribution of microbubbles was maintained at this temperature without affecting the degree of Gd^{3+} binding. Under these conditions, the average Gd^{3+} loading was $3.6 \times 10^7 \pm 1.0 \times 10^7$ ions/microbubble or approximately 40% of the DSPE lipid molecules in the monolayer shell. ICP-OES analysis also determined that negligible amounts of Gd^{3+} bound to lipid-coated microbubbles without DOTA.

Fragmented microbubbles were produced by the removal of the gas core of intact microbubbles through bath sonication and heating. As observed from both the T_1- and T_2- weighted MRI maps, the control DOTA-without Gd^{3+} microbubbles (intact and destroyed) produced an MRI signal response similar to baseline (saline), which did not deviate significantly with an increase in microbubble concentration. The intact Gd^{3+}-bound samples produced similar MR signal intensities as saline and control microbubbles, and the signal intensity was not dependent on an increase in sample concentration. Similarly, it was observed that the relaxation rate did not increase versus increasing intact Gd^{3+}-bound microbubble concentration, and the signal response produced was similar to that of control samples.

The fragmented Gd^{3+}-bound microbubbles, however, resulted in a noticeable increase in MRI signal intensities compared to saline, control and

intact Gd^{3+}-bound microbubbles. Additionally, the effect was concentration-dependent, with an increase in fragmented Gd^{3+}-bound sample concentration leading to an increase in MRI signal intensity. These results suggest that the MR signal came primarily from the Gd^{3+} groups and not the other components of the lipid microbubble shell, and the relaxation rate appeared to be most strongly related to the state of the microbubble (i.e., intact vs. fragmented).

Molar relaxivities (mM^{-1} s^{-1}) were also calculated. The longitudinal molar relaxivity (r_1) increased by ~200% going from fragmented control DOTA-bound microbubbles to fragmented Gd^{3+}-bound microbubbles. The transversal molar relaxivity (r_2) increased by ~300% going from fragmented control DOTA-bound without Gd^{3+}microbubbles to fragmented Gd^{3+}-bound microbubbles. Both r_1 and r_2 for the fragmented Gd^{3+}-bound microbubbles were similarly greater than the corresponding values for the intact Gd^{3+}-bound microbubbles. The average r_1 and r_2 values for the fragmented microbubbles were 4.2×10^8 and 1.3×10^{10} mM^{-1} s^{-1} per microbubble, respectively.

Thus, chelation of the paramagnetic lanthanide Gd^{3+} to the ligand, DOTA, bound on the surface of lipid-shelled microbubbles was achieved at a reaction temperature of 50 ^{o}C without degrading 4-5-μm microbubble size distribution. Under both T_1 and T_2-weighted MRI characterization *in vitro*, the intact microbubble monolayer configuration of the Gd^{3+} -DOTA microbubbles provided MRI signal enhancement similar to baseline saline. However, the liposomes produced from fragmentation of the Gd^{3+} -bound microbubbles resulted in significant increase in the MRI signal. Furthermore, the relaxivity of the resulting Gd^{3+} -bound liposomes were slightly higher than those of commercially available

MRI contrast. The inherent differences in MRI signal intensities between intact and fragmented Gd^{3+}-DOTA bound microbubbles can be beneficial for MRIg-FUS therapy applications.

Although particular configurations have been discussed herein, other configurations can also be employed. Furthermore, the foregoing descriptions apply, in some cases, to examples generated in a laboratory, but these examples can be extended to production techniques. For example, where quantities and techniques apply to the laboratory examples, they should not be understood as limiting. In addition, although the production of oxygen microbubbles has been specifically described herein, other gases (elemental or compositions) are also possible according to one or more contemplated embodiments.

In various embodiments, pre-formed microbubbles can be used as cavitation nuclei to lower the acoustic intensity threshold required for tissue ablation with focused ultrasound therapy (FUS), thereby lowering the thermal buildup in surrounding tissue.

Intravenously administered microbubbles may also be used to enhance vascular permeability for targeted drug and gene delivery. For blood-brain barrier (BBB) opening applications, an MRI-detectable microbubble formulation can be used to measure microbubble concentration, image cavitation events, and to determine the biodistribution of microbubble shell debris following FUS.

In various embodiments, it is disclosed a method and system for using paramagnetic lanthanide-bound microbubbles to spatially and temporally control

a magnetic resonance imaging (MRI) signal via microbubble fragmentation. In other embodiments, using microbubble cavitation as a MRI biosensor is disclosed to monitor and minimize the side effects associated with high intensity focused ultrasound (HIFU).

Various embodiments include a method of controlling an imaging signal through microbubble fragmentation, comprising (including): introducing pre-fabricated microbubbles into a portion of a host; bursting the microbubbles using an external acoustic force; and imaging the portion of the host using an imaging device. The microbubbles can include a paramagnetic inhomogeneity at the gas-liquid interface when intact, and the paramagnetic inhomogeneity can be eliminated by the bursting of the microbubbles. During fragmentation of the microbubbles, the imaging signal changes from a negative contrast to a positive contrast. Therefore, the imaging signal can be controlled based on a state (e.g., intact or fragmented) of the microbubbles.

The imaging signal intensity increases with an increase of the concentration of the fragmented microbubbles. Therefore, the imaging signal intensity can also be controlled by controlling the concentration of a paramagnetic lanthanide bound to the fragmented microbubble membrane.

In various embodiments, the microbubbles include a lipid coated membrane enveloping a fluid, the paramagnetic inhomogeneity being generated by a paramagnetic lanthanide bound to a surface of the lipid-coated membrane. The paramagnetic lanthanide is bound to the surface of the membrane by post-labeling. The post-labeling can include functionalizing the membrane with a macrocyclic ligand and loading the paramagnetic lanthanide through chelation

to the macrocyclic ligand which is conjugated to the membrane. Post-labeling methods may include generating microbubbles with a ligand expressed on a surface for binding with the label and may further include storing the microbubbles for a time such as days or weeks and then reconstituting by diluting a stored cake for post-labeling thereafter.

According to embodiments, microbubbles are generated by flowing a precursor solution into a reaction volume of a continuous flow or batch sonicator and flowing a gas into the reaction volume at a same time. The precursor and gas are ultrasonically agitated to generate a flow of microbubbles with a wider size distribution than a target size distribution. This can be done in a continuous flow arrangement or a batch arrangement according to know engineering principles. The microbubble solution may then be size sorted, for example, using differential flotation column, a batch or continuous centrifuge, or other device. For example, a container may be filled with the generated microbubble solution after filling, isolating size compartments in the container, each compartment containing a different size population of the generated microbubbles. The container may be a rigid container or a flexible bag and compartments may be isolated using a clamp at different heights of the bag. The size-isolated microbubbles may next be concentrated to form a cake. The cake may be stored and the microbubbles may then be recovered by diluting in a solution and post-labeling. The microbubbles may be collapsed under external pressure to strengthen them.

Prior to introducing the microbubbles into the host, the microbubbles can be size-selected to create a batch having a predetermined size range. Note

that, in addition to the column and container methods, the pre-selecting process can comprise collecting the microbubbles in a syringe and applying centrifuging the syringe to separate microbubbles having a predetermined size from other microbubbles.

In various embodiments, a system and method of real-time monitoring of location, intensity and dose of ultrasound energy deposition in a tissue is disclosed, the method comprising: introducing pre-fabricated microbubbles into a portion of a host; bursting the microbubbles using ultrasound; and imaging the portion of the host using an imaging device. The imaging can include visualizing the ultrasound- induced microbubble destruction using magnetic resonance imaging. The microbubbles can include a membrane enveloping a fluid and a material bound to the membrane which is capable of creating a magnetic inhomogeneity at the gas-liquid interfaces of the microbubbles. When the microbubbles are destroyed, the magnetic inhomogeneity disappears and the image changes from a negative to a positive image contrast based on a concentration of the material remaining on the fragmented microbubbles. The paramagnetic lanthanide can include gadolinium Gd^{3+}.

The method can further include monitoring release of a substance included in the microbubbles. The substance can be a medical drug or a gene.

In various embodiments, a method of producing an image is disclosed, comprising: creating a magnetic inhomogeneity at gas-liquid interfaces of size-selected lipid-coated microbubbles by post-labeling; introducing the resulting microbubbles into a portion of a host; and imaging the portion of the host using an electromagnetic scanner.

In various embodiments, a system for producing an image is disclosed, comprising: a microbubble generator to generate lipid-coated microbubbles including a membrane enveloping a fluid and a material bound to the membrane, the material being capable of creating a magnetic inhomogeneity at the gas-liquid interfaces of the microbubbles; and an imaging device to image a portion of a host after insertion of the lipid-coated microbubbles into the host. The imaging device can include an electromagnetic imaging device, such as, but not limited to, a magnetic resonance imaging device. The microbubble generator can include a device that generates microbubbles that envelope a gas and have a membrane material which includes a paramagnetic material such as, but not limited to, gadolinium. The system can further comprise an ultrasound device configured to destroy microbubbles after insertion into the host.

A method of preparing a plurality of paramagnetic material-bound lipid microbubbles, each microbubble having a predetermined size range, is also disclosed. The method can comprise: preparing a plurality of microbubbles, each microbubble including a lipid coated membrane encapsulating a fluid; inserting the lipid-coated microbubbles into a holding device; separating the microbubbles having a size within the predetermined size range from the rest of the microbubbles by applying centrifugation on the holding device; removing the separated microbubbles having the predetermined size range from the holding device; and labeling the separated microbubbles with a paramagnetic material. The labeling can include: functionalizing the membranes of the separated microbubbles with a macrocyclic ligand; and loading the paramagnetic material

through chelation to the macrocyclic ligand which is conjugated to the membranes.

The preparing can further include: acoustically emulsifying a suspension including a mixture of a phospholipid and a lipo-polymer in the presence of an insoluble gas. The emulsifying can include: dissolving the phospholipid in a chloroform/methanol/water mixture; evaporating the mixture to obtain a dried lipid film; hydrating the lipid film with a mixture including filtered phosphate-buffered saline solution (PBS) and the lipo-polymer to obtain a final lipid concentration; heating through sonication the lipid mixture to a temperature above a phase transition temperature of the phospholipid to disperse lipid aggregates into unilamellar liposomes; introducing the insoluble gas over the surface of the lipid mixture; and sonicating the lipid mixture at the gas-liquid interface to generate microbubbles therein.

In various embodiments, an imaging system is disclosed for performing an imaging method as described in any of the methods above. The imaging system can be used for monitoring the treatment of a patient.

In various embodiments, a magnetic resonance imaging guided ultrasound therapy system is disclosed performing an imaging method as described herein. The system can be used for ultrasonic tissue ablation.

Features of the disclosed embodiments may be combined, rearranged, omitted, etc., within the scope of the invention to produce additional embodiments. Furthermore, certain features may sometimes be used to advantage without a corresponding use of other features.

It is, thus, apparent that there is provided, in accordance with the present disclosure, medical imaging contrast devices, methods, and systems. Many alternatives, modifications, and variations are enabled by the present disclosure. While specific embodiments have been shown and described in detail to illustrate the application of the principles of the invention, it will be understood that the invention may be embodied otherwise without departing from such principles. Accordingly, Applicants intend to embrace all such alternatives, modifications, equivalents, and variations that are within the spirit and scope of the present invention.

CLAIMS

1. A method of controlling an imaging signal through microbubble fragmentation, comprising:

fabricating and storing microbubbles at a first time and at a later time, recovering pre-fabricated microbubbles;

introducing pre-fabricated microbubbles into a portion of a host;

bursting the microbubbles using an external acoustic force; and

imaging the portion of the host using an imaging device, wherein,

the microbubbles being configured to include a paramagnetic inhomogeneity at the gas-liquid interface when intact and are further configured such that the paramagnetic inhomogeneity disappears after the bursting of the microbubbles, and

controlling the imaging signal responsively to a state of the microbubbles.

2. The method of claim 1, wherein the state of the microbubbles is characterizable as one of intact and fragmented.

3. The method of claim 1, wherein the imaging includes changing, using a controller, an imaging signal from a negative contrast to a positive contrast responsively to a time of microbubble fragmentation and generating at least one image responsively to at least one of a difference in magnitude of the negative and positive contrast and the rate of change from negative to positive contrast.

4. The method of claim 1, wherein the imaging includes controlling the imaging signal intensity responsively to a concentration of the fragmented microbubbles.

5. The method of claim 4, wherein the imaging includes controlling the imaging signal such that the imaging signal intensity increases with an increase of the concentration of the fragmented microbubbles.

6. The method of claim 4, wherein the controlling is performed responsively to a concentration of a paramagnetic lanthanide bound to the fragmented microbubble membrane.

7. The method of claim 1, wherein the imaging signal includes a magnetic resonance imaging signal and the imaging device includes one of a magnetic resonance imaging device and an ultrasound imaging device.

8. The method of claim 1, wherein the microbubbles include a membrane enveloping a fluid, the paramagnetic inhomogeneity being generated by a paramagnetic lanthanide bound to a surface of the membrane.

9. The method of claim 8, wherein the paramagnetic lanthanide is bound to the surface of the membrane by post-labeling.

10. The method of claim 8, wherein the membrane includes a lipid coating and the paramagnetic lanthanide is bound to the lipid coated membrane by post-labeling.

11. The method of one of claims 9 and 10, wherein the post-labeling includes:

functionalizing the membrane with a macrocyclic ligand; and

loading the paramagnetic lanthanide through chelation to the macrocyclic ligand which is conjugated to the membrane.

12. The method of claim 11, wherein the macrocyclic ligand includes a metal chelating ligand.

13. The method of claim 12, wherein the metal chelating ligand includes one of a 1, 4, 7, 10-Tetraazacyclododecane-1, 4, 7, 10-tetraacetic acid (DOTA), a 1, 4, 7, 10-Tetraazacyclododecane-1, 4, 7, 10-tetraacetic acid monoacid mono (N-hydroxysuccinimide ester) (DOTA-NHS), or a (DTPA).

14. The method of claim 11, wherein the lipid coated membrane includes 1, 2-distearoyl-*sn*-glycero-3-phosphoethanolamine (DSPE).

15. The method of claim 11, further comprising reacting the macrocyclic ligand with a primary amino group on the lipid coated membrane.

16. The method of any one of claims 1-15, wherein the paramagnetic lanthanide includes gadolinium Gd^{3+}.

17. The method of any one of claims 1-15, wherein the controlling of the image signal includes spatial and temporal control.

18. The method of claim 1, wherein prior to introducing the microbubbles into the host, the microbubbles are pre-selected to include microbubbles having a predetermined size.

19. The method of claim 18, wherein the pre-selecting includes:

collecting the pre-fabricated microbubbles into a syringe; and

applying centrifugal force to the syringe to separate microbubbles having a predetermined size from other microbubbles.

20. A method of real-time monitoring of location, intensity and dose of ultrasound energy deposition in a tissue, comprising:

introducing pre-fabricated microbubbles into a portion of a host;

bursting the microbubbles using ultrasound; and

imaging the portion of the host using an imaging device,

the imaging including visualizing the ultrasound- induced microbubble destruction using magnetic resonance imaging,

the microbubbles including a membrane and a material bound to the membrane which is capable of creating a magnetic inhomogeneity at the gas-liquid interfaces of the microbubbles,

the pre-fabricated microbubbles being configured such that the magnetic inhomogeneity disappears after the bursting of the microbubbles,

wherein the image changes from a negative to a positive image contrast based on a concentration of the material remaining on the fragmented microbubble membranes.

21. The method of claim 20, wherein the material includes a paramagnetic lanthanide.

22. The method of claim 21, wherein the microbubbles include a membrane enveloping a fluid, the paramagnetic lanthanide being bound to a surface of the membrane.

23. The method of claim 22, wherein the paramagnetic lanthanide is bound to the surface of the membrane by post-labeling.

24. The method of claim 23, wherein the membrane includes a lipid coating and the paramagnetic lanthanide is bound to the lipid coated membrane by post-labeling.

25. The method of one of claims 24, wherein the post-labeling includes:

functionalizing the membrane with a macrocyclic ligand; and

loading the paramagnetic lanthanide through chelation to the macrocyclic ligand which is conjugated to the membrane.

26. The method of claim 25, wherein the macrocyclic ligand includes a metal chelating ligand.

27. The method of claim 26, wherein the metal chelating ligand includes one of a 1, 4, 7, 10-Tetraazacyclododecane-1, 4, 7, 10-tetraacetic acid (DOTA), a 1, 4, 7, 10-Tetraazacyclododecane-1, 4, 7, 10-tetraacetic acid monoacid mono (N-hydroxysuccinimide ester) (DOTA-NHS), or a (DTPA).

28. The method of claim 27, wherein the lipid coated membrane includes 1, 2-distearoyl-*sn*-glycero-3-phosphoethanolamine (DSPE).

29. The method of claim 27, further comprising reacting the macrocyclic ligand with a primary amino group on the lipid coated membrane.

30. The method of any one of claims 21-29, wherein the paramagnetic lanthanide includes gadolinium Gd^{3+}.

31. The method of claim 21, further including monitoring release of a substance included in the microbubbles.

32. The method of claim 22, wherein the substance is a medical drug.

33. The method of claim 21, wherein prior to introducing the microbubbles into the host, the microbubbles are pre-selected to include microbubbles having a predetermined size.

34. The method of claim 33, wherein the pre-selecting includes:

collecting the pre-fabricated microbubbles into a syringe; and

applying centrifugal force to the syringe to separate microbubbles having a predetermined size from other microbubbles.

35. The method of claim 21, wherein the microbubbles are lanthanide-bound lipid-coated microbubbles.

36. A method of producing an image, comprising:

creating a magnetic inhomogeneity at gas-liquid interfaces of size-selected lipid-coated microbubbles by post-labeling;

introducing the resulting microbubbles into a portion of a host; and

imaging the portion of the host using an electromagnetic scanner.

37. The method of claim 36, wherein the microbubbles include a membrane enveloping a fluid.

38. The method of claim 37, wherein the membrane includes a lipid coating.

39. The method of claim 38, wherein the magnetic inhomogeneity is generated by a paramagnetic material bound to a surface of the lipid coated membrane.

40. The method of claim 39, wherein the paramagnetic material includes a paramagnetic lanthanide.

41. The method of claim 40, wherein the paramagnetic lanthanide is gadolinium Gd^{3+}.

42. The method of claim 39, wherein the post-labeling includes:

functionalizing the membrane with a macrocyclic ligand; and

loading the paramagnetic material through chelation to the macrocyclic ligand which is conjugated to the membrane.

43. The method of claim 42, wherein the macrocyclic ligand includes a metal chelating ligand.

44. The method of claim 43, wherein the metal chelating ligand includes one of a 1, 4, 7, 10-Tetraazacyclododecane-1, 4, 7, 10-tetraacetic acid (DOTA), a 1, 4, 7, 10-Tetraazacyclododecane-1, 4, 7, 10-tetraacetic acid monoacid mono (N-hydroxysuccinimide ester) (DOTA-NHS), or a (DTPA).

45. The method of claim 44, wherein the lipid coated membrane includes 1, 2-distearoyl-*sn*-glycero-3-phosphoethanolamine (DSPE).

46. The method of claim 42, further including reacting the macrocyclic ligand with a primary amino group on the lipid membrane.

47. The method of claim 36, wherein the microbubbles include a membrane enveloping a gas.

48. The method of claim 36, further comprising imaging the same portion of a host using an ultrasound imaging device.

49. The method of claim 36, further comprising destroying the microbubbles using ultrasound.

50. A system for producing an image, comprising:

a microbubble generator to generate lipid-coated microbubbles including a membrane enveloping a fluid and a material bound to the membrane, the material being capable of creating a magnetic inhomogeneity at the gas-liquid interfaces of the microbubbles; and

an imaging device to image a portion of a host after insertion of the lipid-coated microbubbles into the host.

51. The system of claim 50, wherein the imaging device includes an electromagnetic imaging device.

52. The system of claim 51, wherein the electromagnetic imaging device includes a magnetic resonance imaging device.

53. The system of claim 51, wherein the microbubble generator includes a device that generates microbubbles that envelope a gas.

54. The system of claim 51, further comprising an ultrasound device configured to destroy microbubbles after insertion into the host.

55. The system of any one of claims 51-54, wherein the membrane material includes a paramagnetic material.

56. The system of claim 55, wherein the paramagnetic material includes gadolinium Gd^{3+}.

57. The system of claim 55, wherein the microbubble generator includes a device that bounds the paramagnetic material to the lipid-coated membrane by:

functionalizing the membrane with a macrocyclic ligand; and

loading the paramagnetic material through chelation to the macrocyclic ligand which is conjugated to the membrane.

58. The system of claim 57, wherein the macrocyclic ligand includes a metal chelating ligand.

59. The system of claim 58, wherein the metal chelating ligand includes one of a 1, 4, 7, 10-Tetraazacyclododecane-1, 4, 7, 10-tetraacetic acid (DOTA), a 1, 4, 7, 10-Tetraazacyclododecane-1, 4, 7, 10-tetraacetic acid monoacid mono (N-hydroxysuccinimide ester) (DOTA-NHS), or a (DTPA).

60. The system of claim 57, wherein the lipid coated membrane includes 1, 2-distearoyl-sn-glycero-3-phosphoethanolamine (DSPE).

61. The system of claim 57, further including reacting the macrocyclic ligand with a primary amino group on the lipid membrane.

62. A method of preparing a plurality of paramagnetic material-bound lipid microbubbles, each microbubble having a predetermined size range, comprising:

preparing a plurality of microbubbles, each microbubble including a lipid coated membrane encapsulating a fluid;

inserting the lipid-coated microbubbles into a holding device;

separating the microbubbles having a size within the predetermined size range from the rest of the microbubbles by applying centrifugation on the holding device;

labeling the separated microbubbles with a paramagnetic material, wherein the labeling includes:

functionalizing the membranes of the separated microbubbles with a macrocyclic ligand; and

loading the paramagnetic material through chelation to the macrocyclic ligand which is conjugated to the membranes.

63. The method of claim 62, wherein the preparing includes:

acoustically emulsifying a suspension including a mixture of a phospholipid and a lipo-polymer in the presence of an insoluble gas.

64. The method of claim 63, wherein the emulsifying includes:

dissolving the phospholipid in a chloroform/methanol/water mixture;

evaporating the mixture to obtain a dried lipid film;

hydrating the lipid film with a mixture including filtered phosphate-buffered saline solution (PBS) and the lipo-polymer to obtain a final lipid concentration;

heating through sonication the lipid mixture to a temperature above a phase transition temperature of the phospholipid to disperse lipid aggregates into unilamellar liposomes;

introducing the insoluble gas over the surface of the lipid mixture; and

sonicating the lipid mixture at the gas-liquid interface to generate microbubbles therein.

65. The method of claim 62, wherein the holding device is a syringe.

66. The method of claim 62, wherein the predetermined size range includes a diameter range between 4-10 micrometers.

67. The method of claim 62, wherein phospholipid includes 1, 2-distearoyl-sn-glycero-3-phosphoethanolamine (DSPE) and the lipo-polymer includes 1, 2-ditearoyl-sn-glycero-3-phosphoethanolamine-N-[methoxy(polyethylene glycol)-2000] (DPS-PEG2000), and the insoluble gas includes perfluorobutane (PFB).

68. An imaging system performing an imaging method as claimed in any one of claims 1-49 and 62-67.

69. An imaging system for monitoring treatment of a subject performing an imaging method as claimed in any one of claims 1-49 and 62-67.

70. A magnetic resonance imaging guided ultrasound therapy system performing an imaging method as claimed in any one of claims 1-49 and 62-67.

71. The system as claimed in claim 70, used for tissue ablation.

72. A method of monitoring the location, intensity and/or dose of ultrasound energy deposition in a tissue, comprising:

introducing pre-fabricated microbubbles into a portion of a host;

bursting the microbubbles using ultrasound; and

imaging the portion of the host using an imaging device,

the imaging including visualizing the ultrasound- induced microbubble destruction using magnetic resonance imaging,

the microbubbles including a membrane and a material bound to the membrane which is capable of creating a magnetic inhomogeneity at the gas-liquid interfaces of the microbubbles,

the microbubbles being configured such that the magnetic inhomogeneity disappears after the bursting of the microbubbles,

wherein the image changes from a negative to a positive image contrast based on a concentration of the material remaining on the fragmented microbubble membranes.

73. The method of claim 72, wherein the material includes a paramagnetic lanthanide.

74. The method of claim 73, wherein the microbubbles include a membrane enveloping a fluid, the paramagnetic lanthanide being bound to a surface of the membrane.

75. The method of claim 74, wherein the paramagnetic lanthanide is bound to the surface of the membrane by post-labeling.

76. The method of claim 75, wherein the membrane includes a lipid coating and the paramagnetic lanthanide is bound to the lipid coated membrane by post-labeling.

77. The method of one of claims 76, wherein the post-labeling includes:

functionalizing the membrane with a macrocyclic ligand; and

loading the paramagnetic lanthanide through chelation to the macrocyclic ligand which is conjugated to the membrane.

78. The method of claim 77, wherein the macrocyclic ligand includes a metal chelating ligand.

79. The method of claim 78, wherein the metal chelating ligand includes one of a 1, 4, 7, 10-Tetraazacyclododecane-1, 4, 7, 10-tetraacetic acid (DOTA), a 1, 4, 7, 10-Tetraazacyclododecane-1, 4, 7, 10-tetraacetic acid monoacid mono (N-hydroxysuccinimide ester) (DOTA-NHS), or a (DTPA).

80. The method of claim 79, wherein the lipid coated membrane includes 1, 2-distearoyl-*sn*-glycero-3-phosphoethanolamine (DSPE).

81. The method of claim 79, further comprising reacting the macrocyclic ligand with a primary amino group on the lipid coated membrane.

82. The method of any one of claims 21-29, wherein the paramagnetic lanthanide includes gadolinium Gd^{3+}.

83. The method of claim 73, further including monitoring release of a substance included in the microbubbles.

84. The method of claim 74, wherein the substance is a medical drug.

85. The method of claim 73, wherein prior to introducing the microbubbles into the host, the microbubbles are siz-filtered to include microbubbles having a predetermined size range.

86. The method of claim 85, wherein the pre-selecting includes:

collecting the microbubbles into a vessel or flow channel and subjecting to a centrifugal force.

87. The method of claim 73, wherein the microbubbles are lanthanide-bound lipid-coated microbubbles.

88. A method or system as in any of the foregoing embodiments in which size-selection of microbubbles is performed using a flexible container in which compartments are pinched off to isolate strata containing microbubbles having different size ranges.

89. A method or system as in any of the foregoing claims in which size selected microbubbles are generated, formed into a cake by removing non-bubble material and storing the bubbles prior to reconstituting and labeling them.

90. A method or system as in any of the foregoing claims in which a display is generated to show the contrast-enhanced deposition of energy or mass through the detected effect of bursting the labeled microbubbles.

Size distribution of polydisperse microbubbles

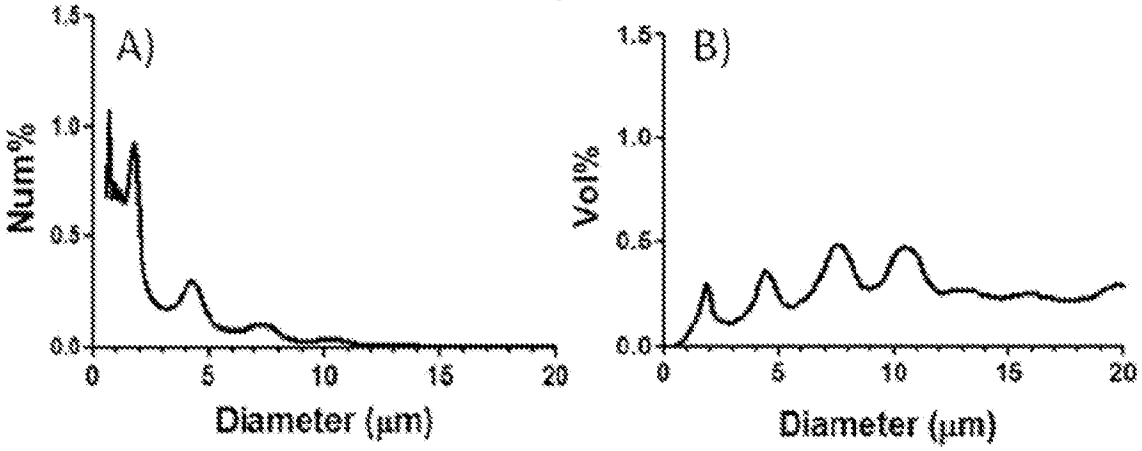

FIG. 1

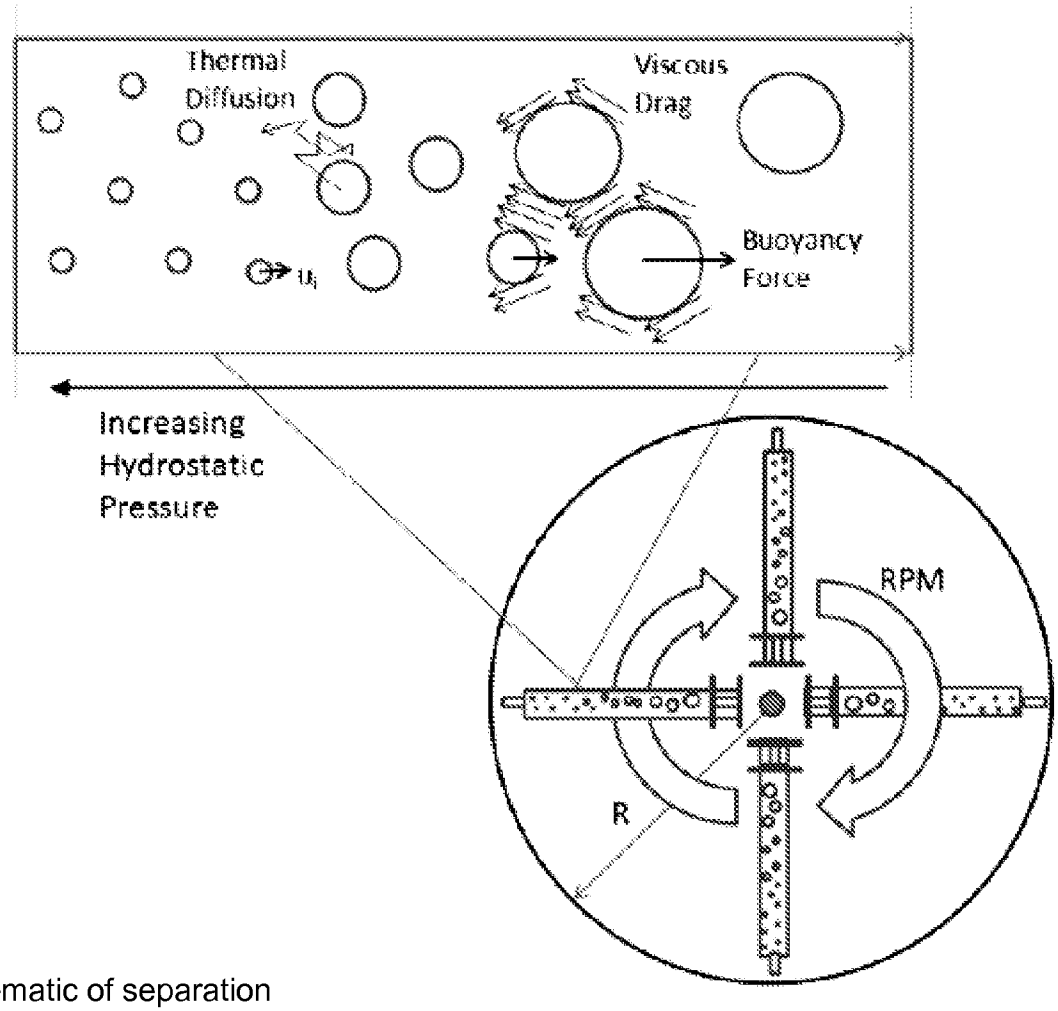

Schematic of separation
by centrifugation

FIG. 2

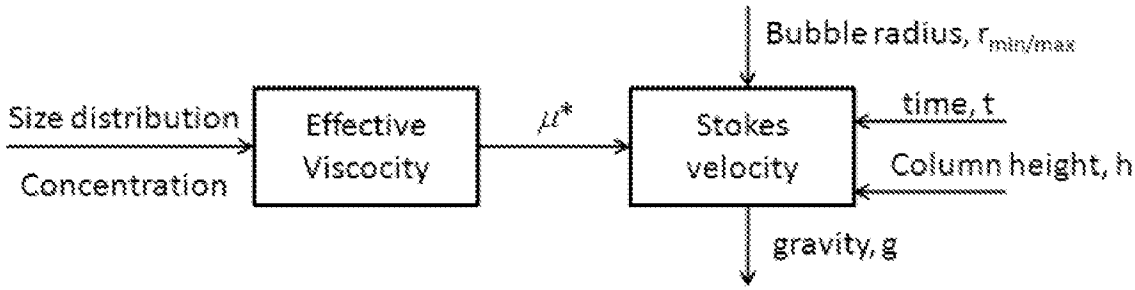
Schematic of Size Isolation Protocol
Bubble radius, $r_{min/max}$
Size distribution
Concentration
Effective Viscocity
μ^*
Stokes velocity
time, t
Column height, h
gravity, g

FIG. 3

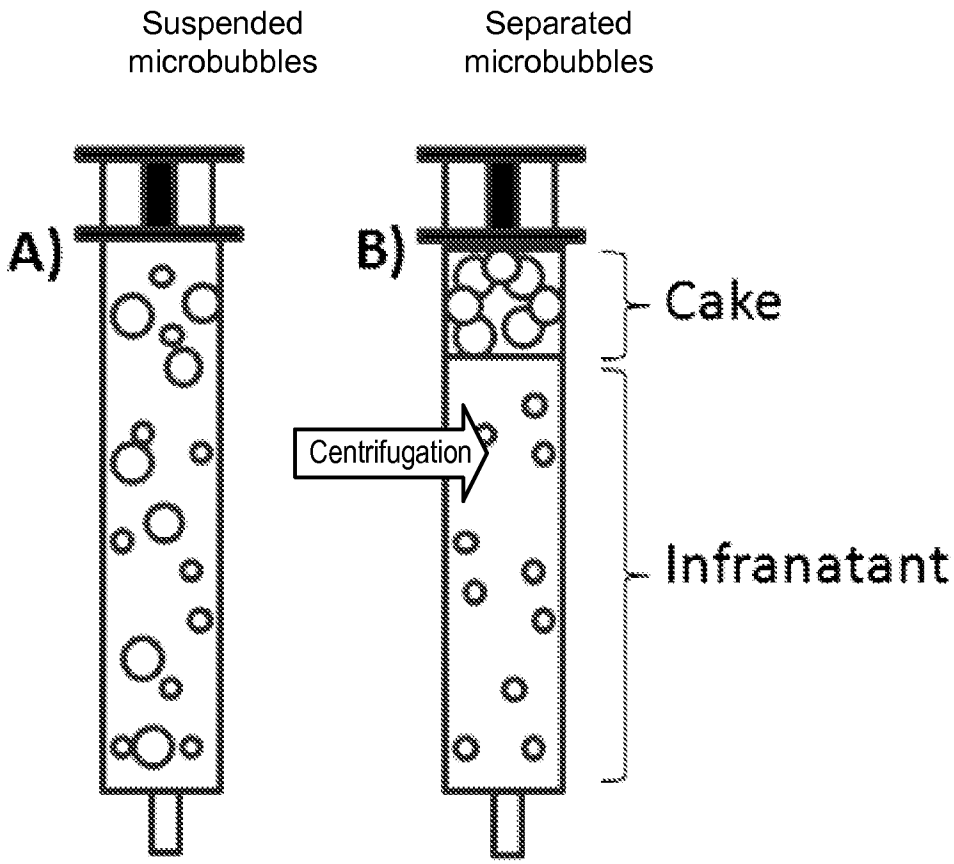
Suspended microbubbles
Separated microbubbles
A)
B)
Cake
Centrifugation
Infranatant

FIG. 4

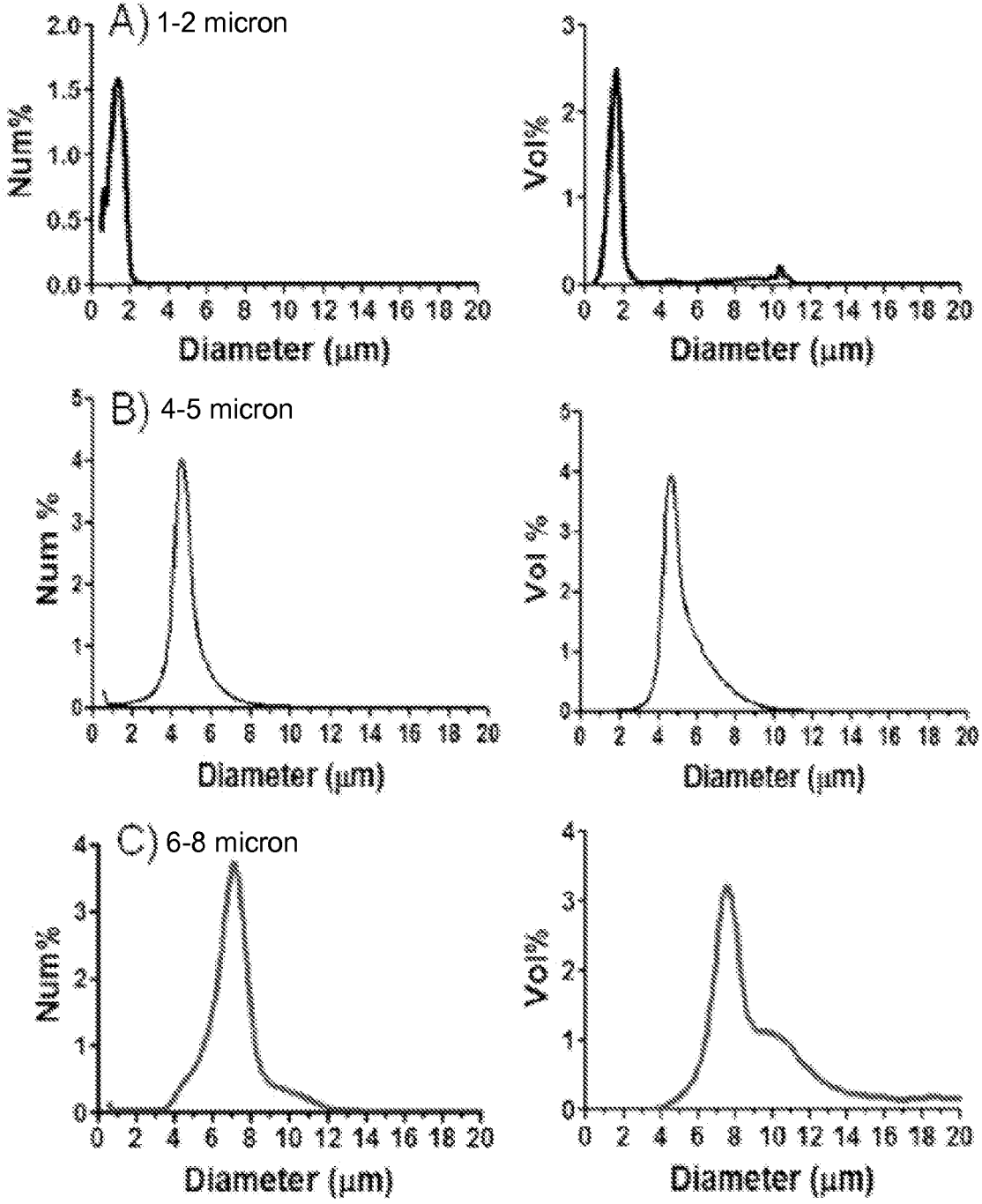
A) 1-2 micron
Num%
Vol%
Diameter (µm)
B) 4-5 micron
Num %
Vol %
Diameter (µm)
C) 6-8 micron
Num%
Vol%
Diameter (µm)

FIG. 5

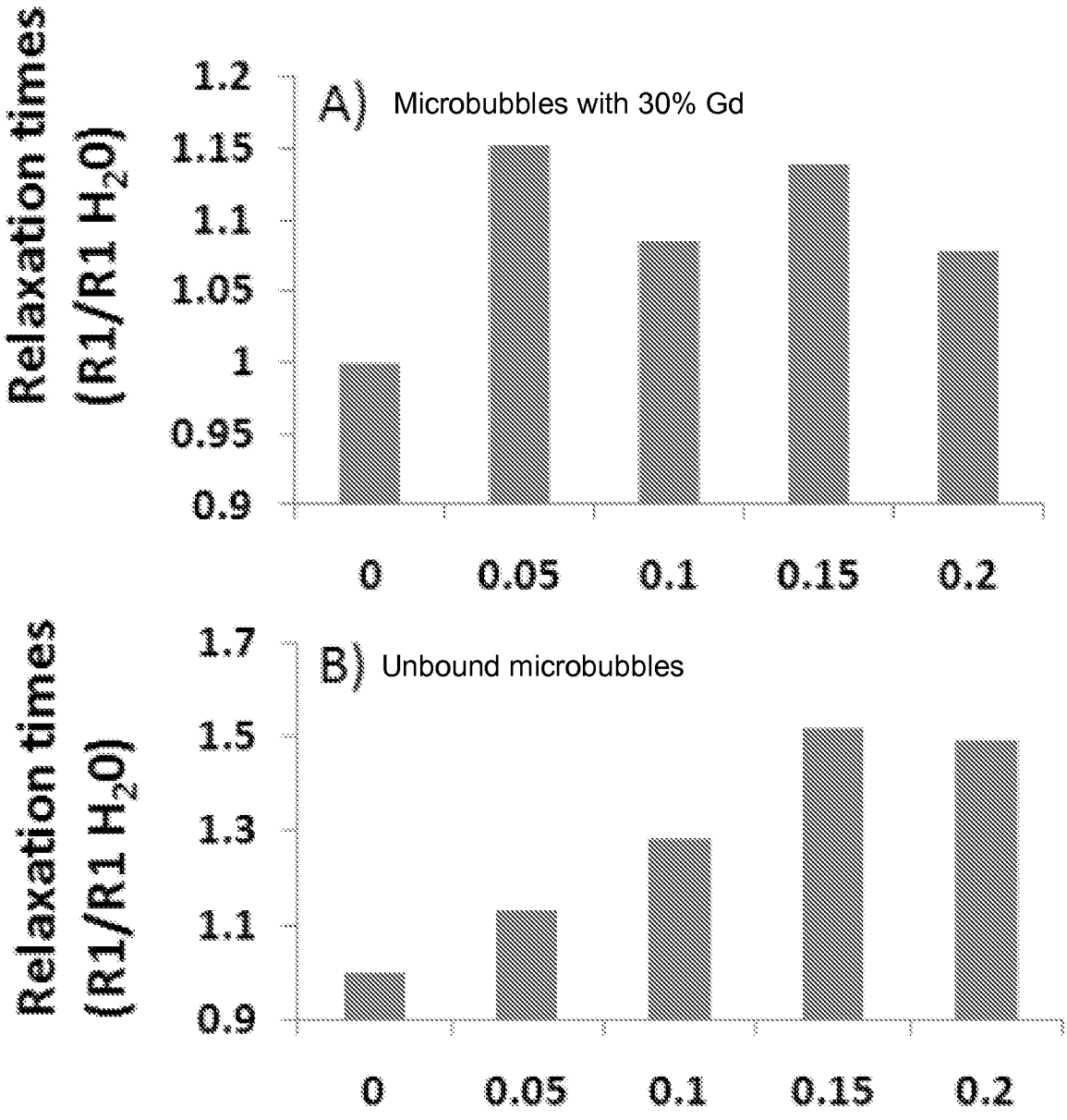
Relaxation times
(R1/R1 H2O)
A) Microbubbles with 30% Gd
1.2
1.15
1.1
1.05
1
0.95
0.9
0
0.05
0.1
0.15
0.2
Relaxation times
(R1/R1 H2O)
B) Unbound microbubbles
1.7
1.5
1.3
1.1
0.9
0
0.05
0.1
0.15
0.2

FIG. 6

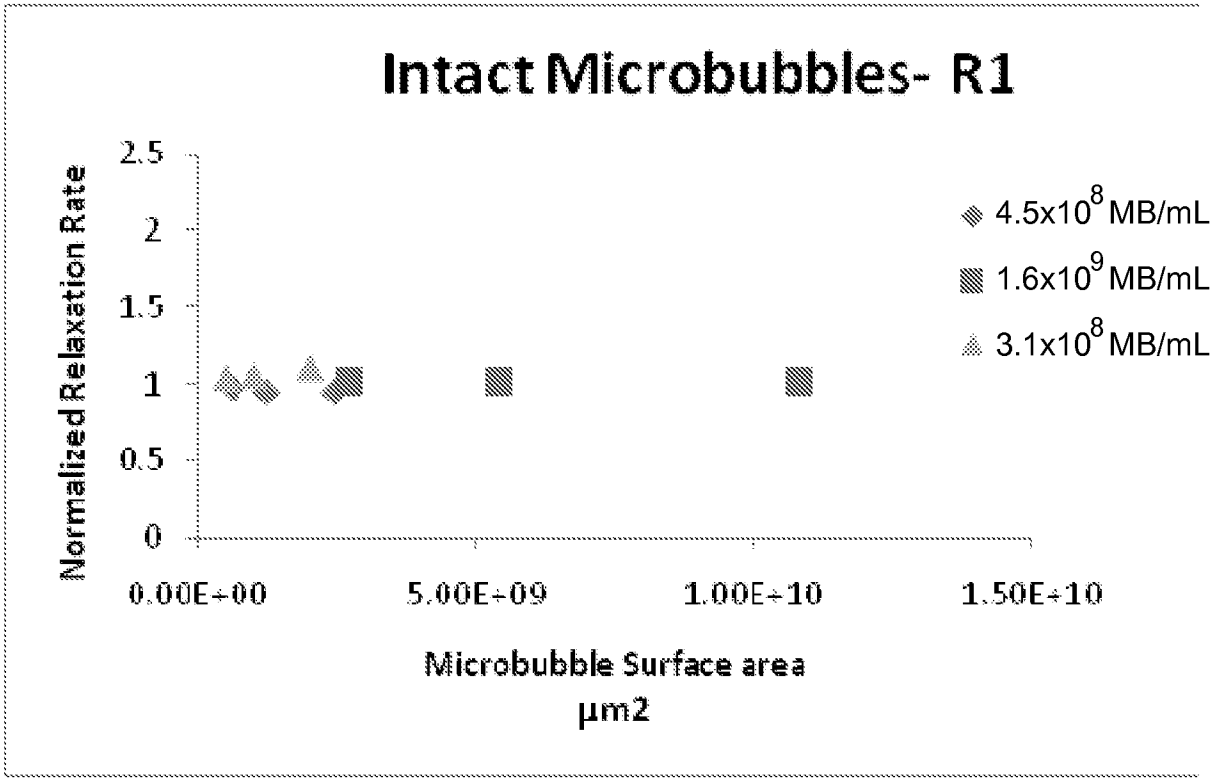
Intact Microbubbles- R1
Normalized Relaxation Rate
2.5
2
1.5
1
0.5
0
0.00E+00
5.00E+09
1.00E+10
1.50E+10
Microbubble Surface area
µm2
4.5x10^8 MB/mL
1.6x10^9 MB/mL
3.1x10^8 MB/mL

FIG. 7A

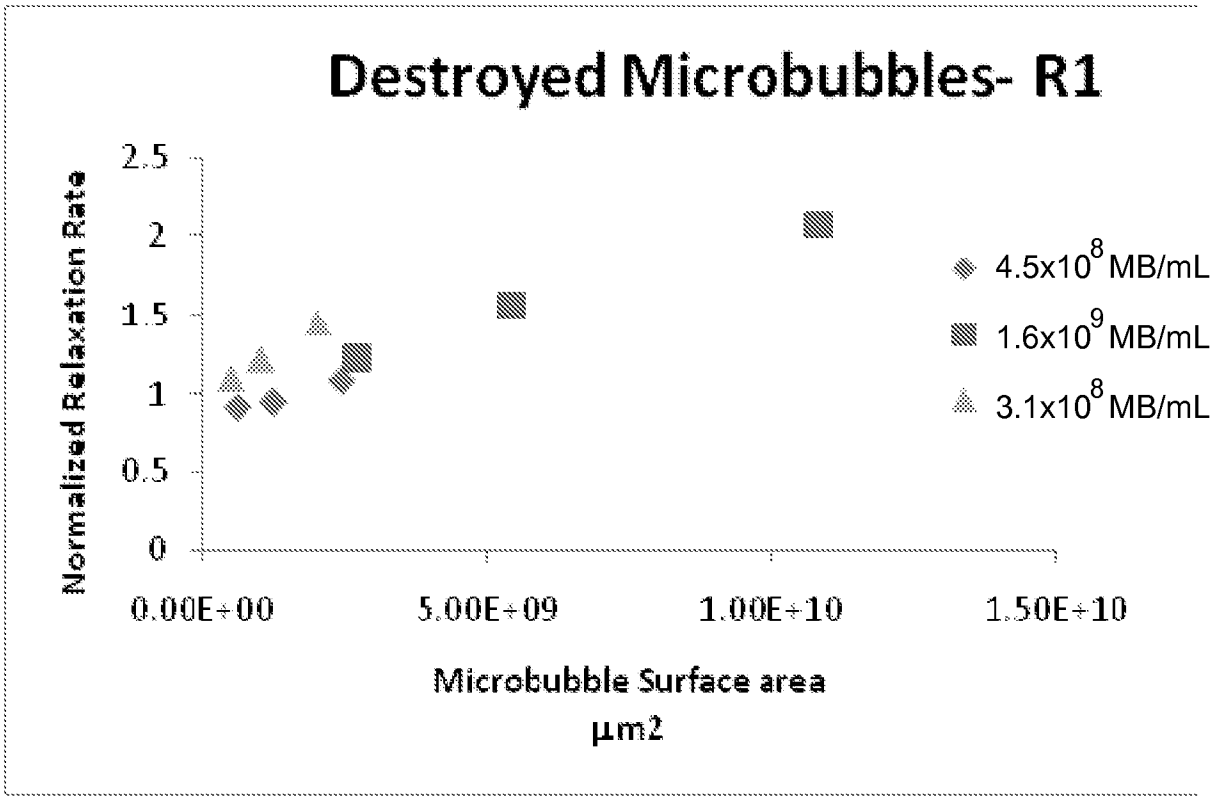
Destroyed Microbubbles- R1
Normalized Relaxation Rate
2.5
2
1.5
1
0.5
0
0.00E+00
5.00E+09
1.00E+10
1.50E+10
Microbubble Surface area
µm2
4.5x10^8 MB/mL
1.6x10^9 MB/mL
3.1x10^8 MB/mL

FIG. 7B

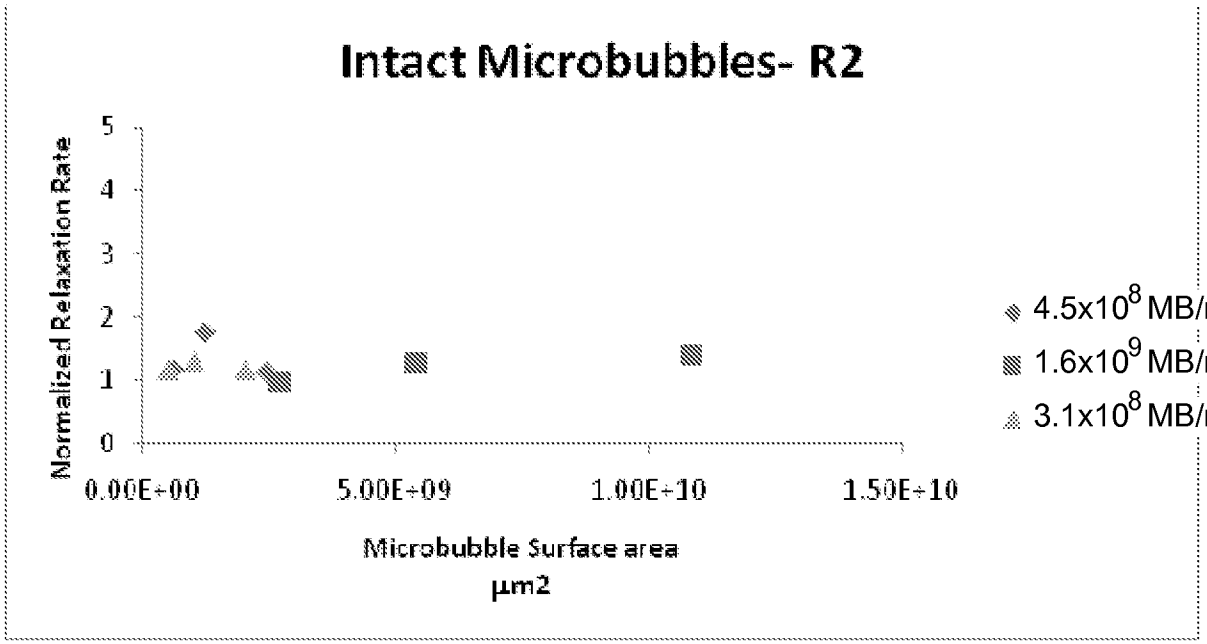
Intact Microbubbles- R2
Normalized Relaxation Rate
0
1
2
3
4
5
0.00E+00
5.00E+09
1.00E+10
1.50E+10
Microbubble Surface area
µm2
4.5x10^8 MB/mL
1.6x10^9 MB/mL
3.1x10^8 MB/mL

FIG. 8A

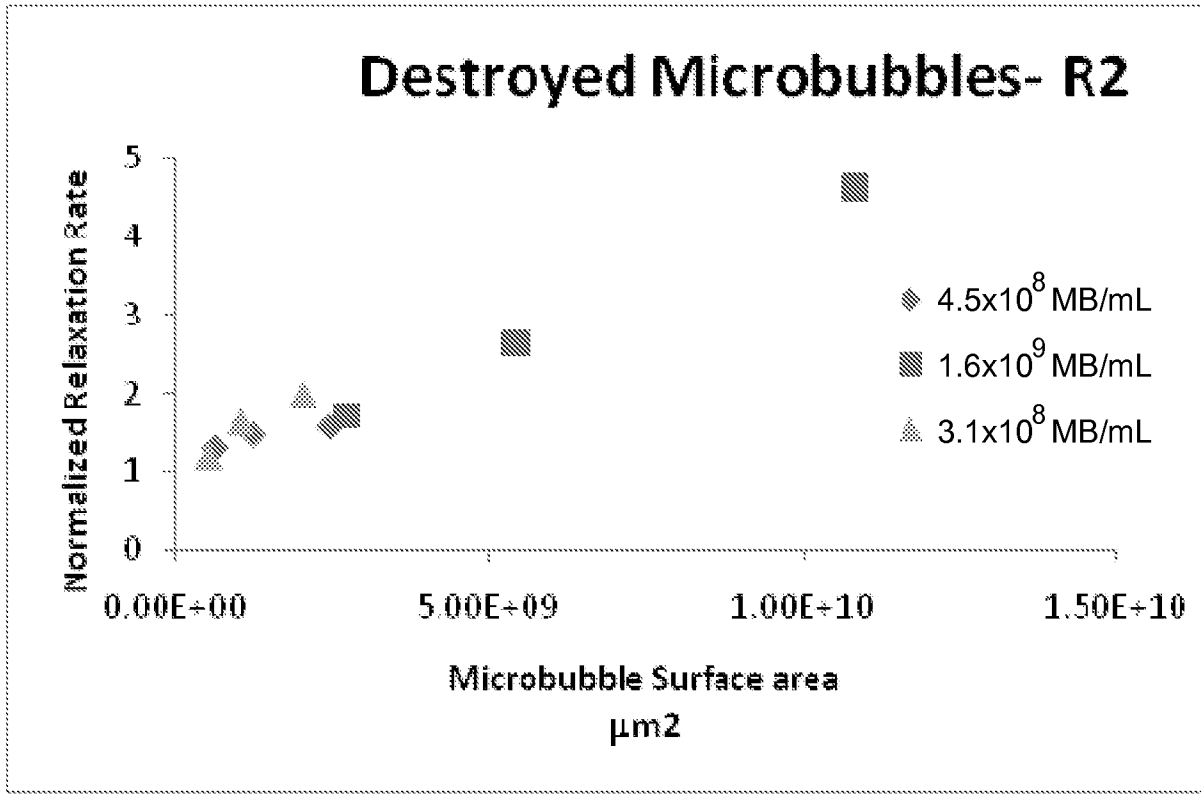
Destroyed Microbubbles- R2
Normalized Relaxation Rate
0
1
2
3
4
5
0.00E+00
5.00E+09
1.00E+10
1.50E+10
Microbubble Surface area
µm2
4.5x10^8 MB/mL
1.6x10^9 MB/mL
3.1x10^8 MB/mL

FIG. 8B

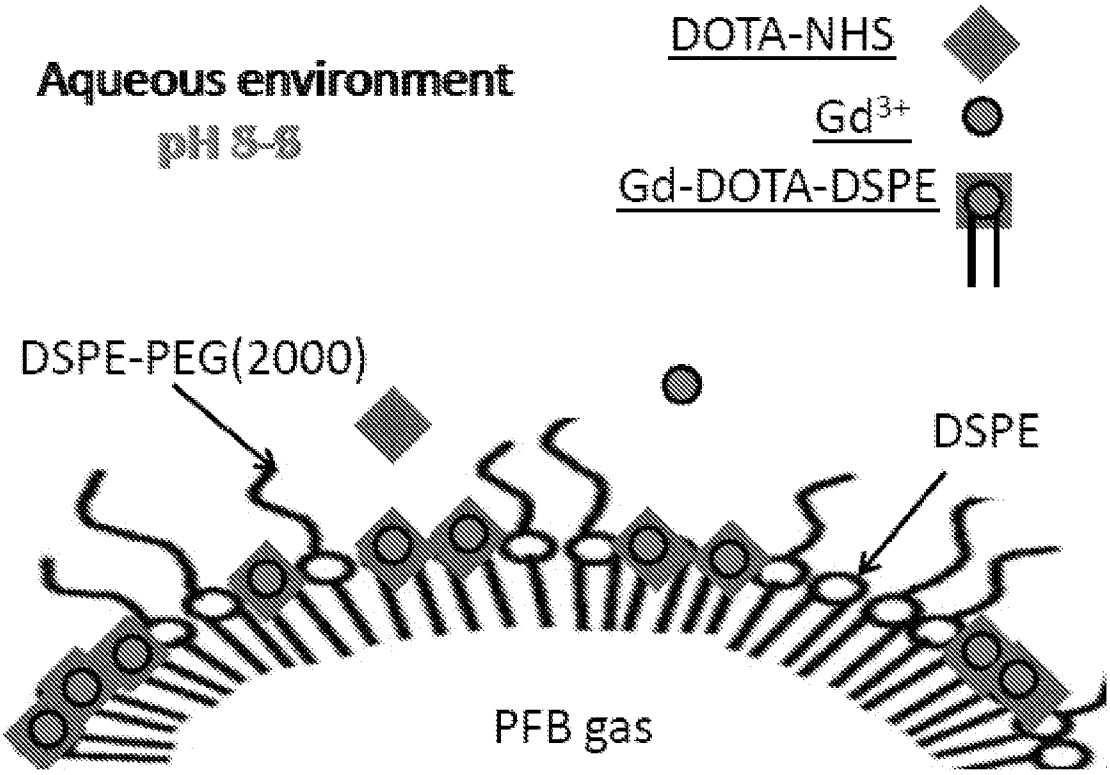
Aqueous environment
pH 5-6
DOTA-NHS
Gd3+
Gd-DOTA-DSPE
DSPE-PEG(2000)
DSPE
PFB gas

FIG. 9

INTERNATIONAL SEARCH REPORT

International application No.
PCT/US 11/46865

A. CLASSIFICATION OF SUBJECT MATTER
IPC(8) - A61B 8/00 (2011.01)
USPC - 424/9.52
According to International Patent Classification (IPC) or to both national classification and IPC

B. FIELDS SEARCHED

Minimum documentation searched (classification system followed by classification symbols)
IPC(8) - A61B 8/00 (2011.01)
USPC - 424/9.52

Documentation searched other than minimum documentation to the extent that such documents are included in the fields searched
USPC - 424/9.363; 534/15,16; 540/465,474

Electronic data base consulted during the international search (name of data base and, where practicable, search terms used)
Databases: USPTO PubWEST(,USPT,EPAB,JPAB); Google Scholar
Search terms: microbubble, liposome, acoustic, ultrasound, MRI, contrast, positive, negative, brightness, intensity, gadolinium, chelation, DOTA, DSPE, DTPA, centrifuge, drug delivery, imaging, kit, paramagnetic, chloroform, water

C. DOCUMENTS CONSIDERED TO BE RELEVANT

Category*	Citation of document, with indication, where appropriate, of the relevant passages	Relevant to claim No.
X -- Y	US 2008/0145311 A1 (LANZA et al.) 19 June 2008 (19.06.2008); para [0009], [0017]-[0122]	36-47, 49-61 --- 1-15, 18-35, 48, 62-67, 72-87
Y	US 2008/0206131 A1 (JAFFRAY et al.) 28 August 2008 (28.08.2008); para [0035]-[0062]	1-15, 18-35, 48, 72-87
Y	US 2005/0201942 A1 (DUGSTAD et al.) 15 September 2005 (15.09.2005); para [0020]-[0054], [0061]-[0098]	19, 34, 62-67, 86
A	US 2007/0081946 A1 (SCHNEIDER et al.) 12 April 2007 (12.04.2007); para [0057]-[0210]	1-15, 18-67, 72-87

☐ Further documents are listed in the continuation of Box C. ☐

* Special categories of cited documents:
"A" document defining the general state of the art which is not considered to be of particular relevance
"E" earlier application or patent but published on or after the international filing date
"L" document which may throw doubts on priority claim(s) or which is cited to establish the publication date of another citation or other special reason (as specified)
"O" document referring to an oral disclosure, use, exhibition or other means
"P" document published prior to the international filing date but later than the priority date claimed
"T" later document published after the international filing date or priority date and not in conflict with the application but cited to understand the principle or theory underlying the invention
"X" document of particular relevance; the claimed invention cannot be considered novel or cannot be considered to involve an inventive step when the document is taken alone
"Y" document of particular relevance; the claimed invention cannot be considered to involve an inventive step when the document is combined with one or more other such documents, such combination being obvious to a person skilled in the art
"&" document member of the same patent family

Date of the actual completion of the international search	Date of mailing of the international search report
14 December 2011 (14.12.2011)	05 JAN 2012
Name and mailing address of the ISA/US Mail Stop PCT, Attn: ISA/US, Commissioner for Patents P.O. Box 1450, Alexandria, Virginia 22313-1450 Facsimile No. 571-273-3201	Authorized officer: Lee W. Young PCT Helpdesk: 571-272-4300 PCT OSP: 571-272-7774

Form PCT/ISA/210 (second sheet) (July 2009)

INTERNATIONAL SEARCH REPORT

International application No.
PCT/US 11/46865

Box No. II Observations where certain claims were found unsearchable (Continuation of item 2 of first sheet)

This international search report has not been established in respect of certain claims under Article 17(2)(a) for the following reasons:

1. ☐ Claims Nos.:
because they relate to subject matter not required to be searched by this Authority, namely:

2. ☐ Claims Nos.:
because they relate to parts of the international application that do not comply with the prescribed requirements to such an extent that no meaningful international search can be carried out, specifically:

3. ☒ Claims Nos.: 16-17, 68-71, and 88-90
because they are dependent claims and are not drafted in accordance with the second and third sentences of Rule 6.4(a).

Box No. III Observations where unity of invention is lacking (Continuation of item 3 of first sheet)

This International Searching Authority found multiple inventions in this international application, as follows:

1. ☐ As all required additional search fees were timely paid by the applicant, this international search report covers all searchable claims.

2. ☐ As all searchable claims could be searched without effort justifying additional fees, this Authority did not invite payment of additional fees.

3. ☐ As only some of the required additional search fees were timely paid by the applicant, this international search report covers only those claims for which fees were paid, specifically claims Nos.:

4. ☐ No required additional search fees were timely paid by the applicant. Consequently, this international search report is restricted to the invention first mentioned in the claims; it is covered by claims Nos.:

Remark on Protest

☐ The additional search fees were accompanied by the applicant's protest and, where applicable, the payment of a protest fee.

☐ The additional search fees were accompanied by the applicant's protest but the applicable protest fee was not paid within the time limit specified in the invitation.

☐ No protest accompanied the payment of additional search fees.